Ray tracing/correlation approach to estimation of surface-based duct parameters from radar clutter*

Zhao Xiao-Feng(赵小峰), Huang Si-Xun(黄思训)†, and Sheng Zheng(盛 峥)

Institute of Meteorology, PLA University of Science and Technology, Nanjing 211101, *China*

(Received 1 June 2009; revised manuscript received 3 September 2009)

This paper describes a technique to estimate surface-based duct parameters by using a simple ray tracing/correlation method. The approach is novel in that it incorporates the Spearman rank-order correlation scheme between the observed surface clutter and the surface ray density for a given propagation path. The simulation results and the real data results both demonstrate the ability of this method to estimate surface-based duct parameters. Compared with the results obtained by a modified genetic algorithm combined with the parabolic wave equation, the results retrieved from the ray tracing/correlation scheme show a minor reduction in accuracy but a great improvement on computation time. Therefore the ray tracing/correlation method might be used as a precursor to more sophisticated and slower techniques, such as genetic algorithm and particle filters, by narrowing the parameter search space and providing a comprehensive and more efficient estimation algorithm.

Keywords: ray tracing, Spearman rank correlation, surface-based duct, radar clutter

PACC: 9260V

1. Introduction

Determination of microwave propagation conditions in the troposphere is important for assessing the performance of both communications and radar systems.[1] Conventional methods of estimating modified refractivity, $M(z) = 10^6 \times (n - 1 + z/a_e)$, where z represents the height, n is the refractive index and a_e is the Earth's radius, can be divided into two categories: (i) direct sensing techniques which involve the measuring of atmospheric pressure, temperature and humidity to determine the index of refraction;[2] and (ii) remote sensing techniques which infer refractivity more indirectly. Great advances have been made recently in remotely sensing refractivity parameters from radar sea clutter,[3−7] of which the forward model is based on the split-step Fourier parabolic wave equation (PWE) algorithm. One of the advantages of PWE is that it is particularly well suited for range-dependent refractivity profiles. However, a significant disadvantage is that it requires an extensively computational source, which increases with frequency, antenna beam width, and altitude increasing, of which the results are desired.

Ray tracing models have gained special attention in the last decade.[8−10] The most attractive aspect for the ray tracing propagation model is that it can find a fast computational way to specify the dominant ray paths that account for the field strength prediction. The technique applied in our estimation procedure is conceptually simple and straightforward. It relies purely on geometrical ray tracing and uses a rank, or nonparametric, correlation scheme between the observed clutter power and ray density at the surface to determine the maximum likelihood estimate of the duct parameters.

2. Surface-based duct refractivity model

Although the marine atmospheric boundary layer variability which causes microwave ducting is often complex in nature, for the purpose of propagation studies, it is often represented at a given range by trilinear and/or bilinear refractivity profiles for surface-based duct (SBD).[11] A tri-linear refractivity profile consists of three basic parameters: base height, trapping layer thickness, and M-deficit (see Fig. 1(a)). Base height is defined as the height from the surface to the lower boundary of the trapping layer. Thickness is defined as the distance between the lower and the upper boundaries of the trapping layer. M-deficit is the difference in modified refractivity value between the

*Project supported by the National Natural Science Foundation of China (Grant No. 40775025).

†Corresponding author. E-mail: huangsxp@yahoo.com.cn

© 2010 Chinese Physical Society and IOP Publishing Ltd

two boundaries of the trapping layer. Base height, thickness and M-deficit determine the height of the duct in the troposphere and the number of rays that would be trapped in the duct. In addition, they also affect the curvature of rays in the trapping layer.[4] If the value of base height reduces to zero, the tri-linear profile will end up with a bilinear profile, (see Fig. 1(b)), which means that the bottom of the duct touches the ground.

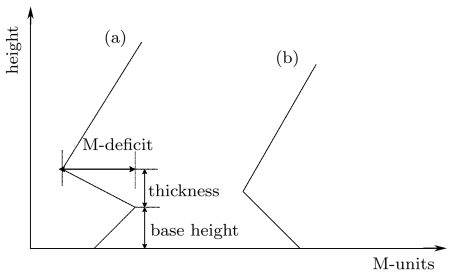


Fig. 1. Surface-based duct refractivity profiles obtained from the tri-linear refractivity model (a) and the bilinear refractivity model (b).

The tri-linear refractivity profile created consists of four height-and-M-unit pairs, which are computed by using the following equation:[12]

$$M(z_i) = M_i = M_{i-1} + \left.\frac{\mathrm{d}M}{\mathrm{d}z}\right|_i (z_i - z_{i-1}),$$
$$i = 1, 2, 3, \qquad (1)$$

where $z_0 = 0$ is the height at mean sea level, the corresponding M-unit value is $M_0 = 339$ M-units, $\mathrm{d}M/\mathrm{d}z|_1 = 0.13$ M-units/m, and $\mathrm{d}M/\mathrm{d}z|_3 = 0.118$ M-units/m. The height above the duct is chosen arbitrarily. For simulation cases, 1000 m is selected.

3. Ray tracing and rank correlation

3.1. Ray tracing approach

The ray tracing model is based on a small angle approximation to Snell's law. For a given vertical refractivity profile defined by a series of heights and corresponding M-unit values, the ray trajectory is determined by successive 'traces' through each of the height/M-unit levels until the desired receiver range or height is reached. As described in Ref. [13], a single step of the ray tracing method could be summarized below. The elevation angle at the end of the step, α_1, is given by,

$$\alpha_1 = \sqrt{\alpha_0^2 + 2 \times 10^{-6}(M_{i+1} - M_i)}, \qquad (2)$$

where α_0 is the elevation angle at the beginning of the step, and M_i and M_{i+1} represent M-unit values at the beginning and end of the step respectively. Increment ΔX and spreading increment ΔS over the step are given as

$$\Delta X = (\alpha_1 - \alpha_0)/g_i,$$
$$\Delta S = (\alpha/\alpha_1 - \alpha/\alpha_0)/g_i,$$
$$g_i = 10^{-6}(M_{i+1} - M_i)/(z_{i+1} - z_i), \qquad (3)$$

where α is the elevation angle at the transmitter, and z_i and z_{i+1} are the heights at the beginning and end of the step respectively. While there is no magnitude or phase associated with the geometrical ray trace used here, the density of rays striking the ground within any particular range interval is a good indicator of the proportionate field strength illuminating the ground and being backscattered.

Two tri-linear refractivity profiles consist of different parameters and are indicated in Fig. 2. The solid profile represents a 350-m SBD created from values of base height, trapping layer thickness, and M-deficit of 300 m, 50 m and 50 M-units, respectively; and the corresponding values of the 100-m SBD (dash-dot line) are 50 m, 50 m and 10 M-units. In order to illustrate the relationship between field strength and ray density, a parabolic equation model as described in Ref. [14] is used to produce synthetic clutter. Figure 3(a1) is the propagation loss coverage diagram computed by the APM software package with the 350-m SBD profile, and the corresponding values at the surface are shown in Fig. 3(a2). The radar is operating at a frequency of 5.6 GHz with an antenna height of 27 m above mean sea level. Five hundred rays were traced in launch angles ranging from a minimum of -0.5° to a maximum of 0.5° (with a launch angle increment of 0.002°) to encompass rays that lie within the critical angle determined by the duct. The critical angle Φ_c is defined as

$$\Phi_\mathrm{c} = \pm\sqrt{2 \times 10^{-6}(M_0 - M_\mathrm{min})}, \qquad (4)$$

where M_0 is the value of M-unit at the antenna height, and M_min is the minimum value of M-unit at all heights. The idea is, of course, that wave fronts radiated at ray angles outside the critical angle will not contribute to surface clutter seen in extended ranges. Figure 3(b1) shows ray tracing paths with the 350-m SBD, and Fig. 3(c1) with the 100-m SBD. Once ray

tracing has been performed the ray density is computed by simply counting the number of 'ray hits' on the surface per range bin, which here is chosen to be approximately 1000 m. The ray density corresponding to Fig. 3(b1) is shown in Figs. 3(b2), 3(c1) and 3(c2).

From similarities in the locations of peaks and lows between Figs. 3(a2) and 3(b2), it follows evidently that there is a strong relationship between regions of high return clutter power and regions of high ray density as well as low clutter and low ray density. A comparison between Fig. 3(a2) and Fig. 3(c2) shows that the relation between clutter power and ray density is poor, because of the different SBD parameters. The rank correlation coefficients will be given in the following section.

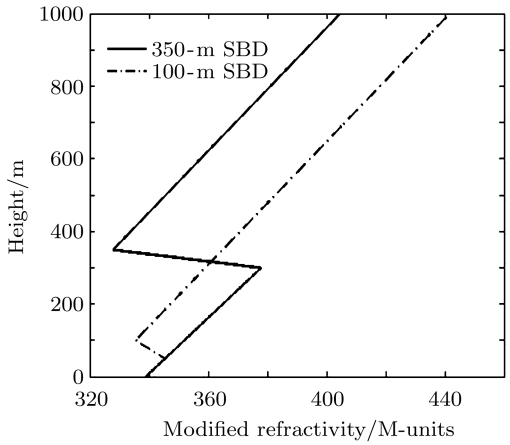


Fig. 2. Tri-linear profiles of 350-m SBD and 100-m SBD.

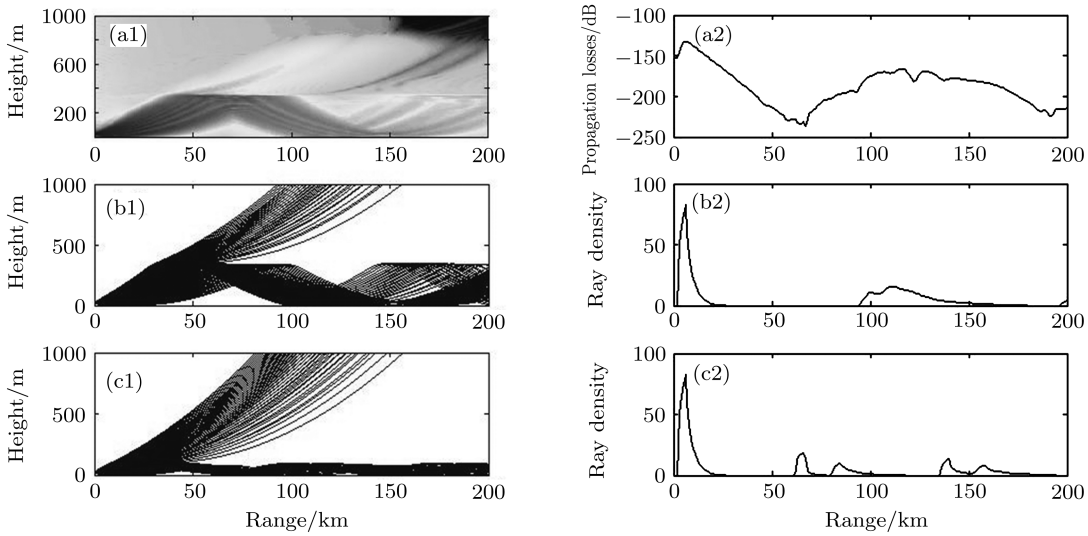


Fig. 3. (a1) Propagation loss coverage diagram based on a 350-m SBD; (a2) The corresponding values at the surface shown in (a1); (b1) Ray tracing trajectories in the presence of a 350-m SBD; (b2) Ray density of (b1) over 1000 m range bin; (c1) Ray trace trajectories in the presence of a 100-m SDB; (c2) Ray density of (c1) over 1000-m range bin.

It should be pointed out that here a small angle approximation is applied to Snell's law in order to reduce the computation time. A ray tracing approach without approximation was developed by Yan *et al.*[1] and the integrator was contained in the 'shaomf' software package. Adopting the 'shaomf' software package to realize ray tracing will be the primary work in our future work.

3.2. Spearman rank-order correlation

Once the ray density is computed for a given refractivity profile, the rank correlation coefficient between ray density and observed clutter signal is determined. The concept behind using rank correlation is that one can 'rank' two data sets that are different in physical meaning, resulting in two uniformly distributed data sets where their correlation can then be obtained. The rank correlation is preferred to linear, or parametric, correlation for several reasons. Unlike the linear correlation, if a high coefficient is determined by using the rank correlation, then it truly exists and any relationship between data samples can be correctly interpreted. The rank correlation is also more robust in the sense that it is resistant to un-

planned defects in the data.[12] The Spearman rank-order correlation coefficient was used for the estimation method presented here.

Let $\boldsymbol{P} = \{p_1, \ldots, p_m\}$ and $\boldsymbol{Q} = \{q_1, \ldots, q_m\}$ denote the ranks of $\{X_1, \ldots, X_m\}$ and $\{Y_1, \ldots, Y_m\}$, respectively. The expression of the Spearman rank-order correlation coefficient R could be expressed as[15]

$$R = 1 - \frac{6\sum (p_i - q_i)^2}{m(m^2-1)}, \quad i = 1, \ldots, m. \tag{5}$$

The rank correlation coefficient between Fig. 3(a2) and Fig. 3(b2) is 0.69, and that between Fig. 3(a2) and Fig. 3(c2) is 0.16, which shows a strong relationship between clutter returns and ray density based on the same refractivity profile.

A flow chart of the ray tracing/correlation (RTC) approach for the estimation of surface-based duct parameters from radar clutter is shown in Fig. 4, where $R_{\max}$ is the maximum rank-order correlation coefficient between the observed clutter power and ray density at the surface, $\boldsymbol{P}$ is the rank of the power of radar clutter and $\boldsymbol{Q}$ is the rank of the ray density at the surface, R_i is the Spearman rank-order correlation coefficient between the observed clutter power and the ray density at the surface which is computed by the parameters of surface-based duct M_i.

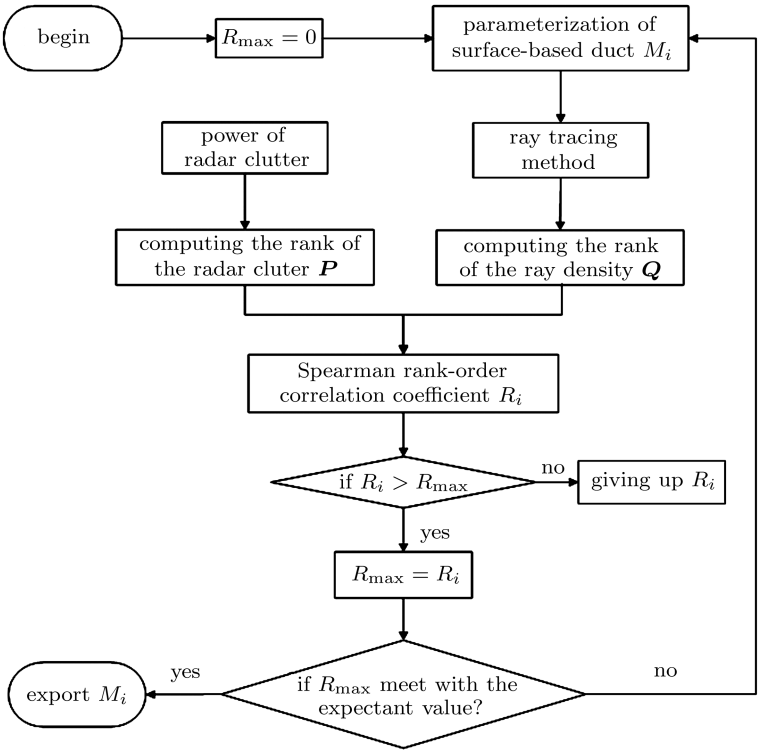


Fig. 4. Flow chart of RTC for the estimation of surface-based duct parameters from radar clutter.

4. Numerical experiment

4.1. Simulation results

For this simulation we begin with a tri-linear 350-m SBD profile described in Subsection 3.1. The refractivity profile will be used to produce our synthetic clutter as shown in Fig. 3(a2), using a parabolic equation model. The tri-linear profile will be the target refractivity profile that we will estimate.

The interested space considered here is 200 km in range and 1000 m in height. The range increment is 1000 m and the height increment is 0.3 m. Since only the values near the surface are used, there will be 200 points in the range being calculated. Let $\{X_1, \ldots, X_{200}\}$ denote the synthetic clutter values at the surface and, $\boldsymbol{P} = \{p_1, \ldots, p_{200}\}$ are the ranks of $\{X_1, \ldots, X_{200}\}$. Let $\{Y_1, \ldots, Y_{200}\}$ denote the number of "ray hits" on the surface per range bin, and $\boldsymbol{Q} = \{q_1, \ldots, q_{200}\}$ are the ranks of $\{Y_1, \ldots, Y_{200}\}$. In

practice, based on the interested space and computation accuracy, we could change the number of the separated points.

Over 6000 refractivity profiles are created based on the information provided in Table 1 which gives the search bounds for SBD tri-linear profile parameters.[12]

Table 1. Search bounds for tri-linear profile parameters.

parameter	lower bound	upper bound	increment
base height/m	1	700	25
M-deficit/M-units	10	150	10
thickness/m	10	150	10

We can now consider rank correlation between ray density and synthetic clutter. The highest rank-order correlation coefficient is 0.71, and the corresponding parameters are base height 275 m, trapping layer thickness 30 m, and M-deficit 40 M-units. Here we should pay attention to an oddity that the highest rank correlation coefficient is even higher than the perfect matching profile (0.69), which shows that this method may not be used for accurate estimation. Table 2 gives the inversion results and computation time retrieved by RTC and the modified genetic algorithm for parabolic wave equation (PWE/MGA).[16] Our computation source is equipped with a Pentium 4 3.0 CPU and 1 GB EMS memory, and operates in the Windows XP system. From Table 2 it is clearly seen that with the same computation time (1205 seconds), though the results from RTC are not accurate enough, they could be used to approximately describe real atmospheric conditions. Yet the quality of PWE/MGA is poor. However, with a longer inversion time, the results from PWE/MGA could be evolved perfectly.

Table 2. Comparison between RTC and PWE/MGA.

	base height/m	M-deficit/M-units	thickness/m	time/s
true value	300	50	50	——
RTC	275	40	30	1205
PWE/MGA	377.1	24.2	47.2	1205
PWE/MGA	309.2	48.5	44.1	6532

4.2. Analysis of different height increments

It is assumed that the modified index of refraction is constant between two fixed layers, which will inevitably cause some errors in computation. As equations (2) and (3) show, the smaller the height bin is selected to be, the smaller the error in computation will be, and at the same time, the longer the computation time consumed will be. In order to find the optimal height bin, i.e. more accurate and less computing, we will divide the vertical height into 10 different types. The height bin is changed from 0.1 m to 1 m. The above 350-m tri-linear profile is taken as an example. For the sake of saving computation time and more accurate estimation, the search bounds and increments for SBD tri-linear profile parameters are changed. The lower bound, the upper bound and the increment for base height are 250 m, 350 m and 5 m, respectively. The corresponding values for M-deficit are 20 M-units, 80 M-units and 5 M-units, and those for thickness are 20 m, 80 m and 5 m, respectively.

Table 3 gives the inversion results by RTC for different height bins, from which we can see that with the increase of the atmosphere layers, the accuracy of the retrieved values is indicated to have a little improvement. The computation time for 1.0 m is 194 s and for 0.1 m is 1939 s. For SBD, the base height and M-deficit are

Table 3. Inversion results obtained by RTC for different height bins.

height bin/m	base height/m	thickness/m	M-deficit/M-units	coefficient	time/s
1.0	270	35	40	0.682	194
0.9	270	35	40	0.682	216
0.8	270	35	40	0.682	243
0.7	270	35	40	0.701	277
0.6	275	35	40	0.713	323
0.5	275	35	40	0.713	387
0.4	275	35	40	0.718	485
0.3	280	35	40	0.762	647
0.2	280	35	40	0.764	971
0.1	280	35	45	0.773	1939

the most important parameters for the magnitude of the ducted field,[4] so we select 0.3 m as an optimal value for the height bin.%vs2mm

4.3. Real data results

To better gauge the performance of RTC by using actual clutter measurements, we will now use clutter data taken from the Space Range Radar from Wallops Island, Virginia. Reference data are acquired from range-dependent refractivity profiles obtained with a helicopter. The clutter map presented here (Fig. 5(a)) is obtained from the surface-based ducting event that occurred on 2 April 1998. The radar is 30.78 m above mean sea level and operates at a frequency of 2.84 GHz. The clutter return values along an azimuthal angle of 150° and 10–60 km in range extracted from Fig. 5(a) are shown in Fig. 5(b). The helicopter measurements at different ranges are shown in Fig. 6 with thin solid lines, from which we can see that the refractivity varies a little in the horizontal direction, so the assumption that the environment is horizontally homogeneous is reasonable. The mean helicopter profile in range is denoted with a thick solid line. The inversion profiles retrieved from RTC and PWE/MGA are shown with a dash-dot line and dash line respectively. The height bin is selected to be 0.3 m. The highest rank correlation coefficient of RTC is 0.80 and the computation time is 737 s, while the time of PWE/MGA is 5430 s. For further information on the radar and the helicopter data, refer to the work by Gerstoft *et al.* [2003].

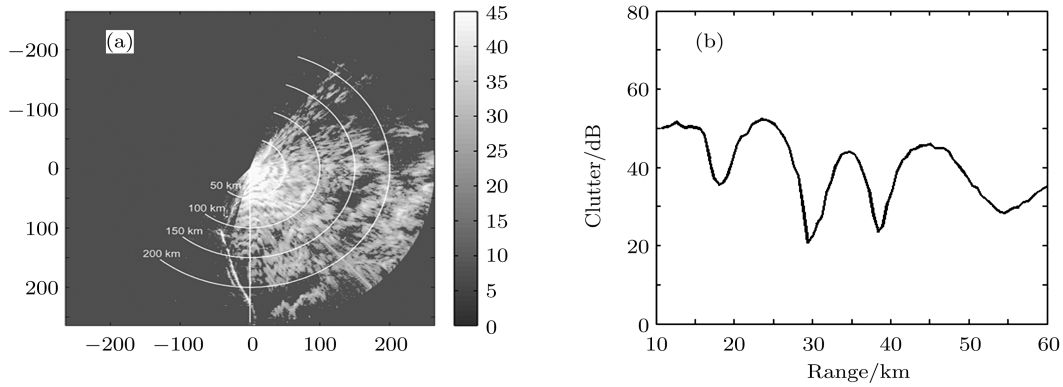


Fig. 5. (a) Clutter map from the Space Range Radar at Wallops Island, VA (Gerstoft *et al.* 2003), and (b) the clutter return as observed by the radar data.

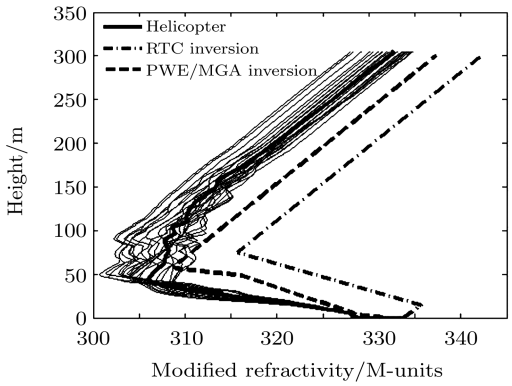


Fig. 6. Refractivity profiles, observed profiles measured from helicopter over ranges (thin solid thin lines), mean helicopter profile (thick solid line), RTC inversion profile (dash-dot line), and PWE/MGA inversion profile (dash line).

4.4. Discussion of numerical experiments

PWE/MGA for a parabolic equation is an inverse problem for detailed values of clutter returns, while the RTC scheme only concerns the rank-order correlation between observed clutter signal and ray density. Since there is little influence of the noise ingredients on the rank-order of radar clutter arrays observed in calm sea or smooth land environments, the observed clutter could be directly used for inversion without further processing, which makes RTC intuitively simple and straightforward.

Both simulation and real data cases have shown the quality of RTC for SBD parameter estimation.

The results of RTC show that little accuracy is lost compared with PWE/MGA. However, the computational time of PWE/MGA is very long, whereas that of RTC is in real time. Different height bins could bring about different computation accuracies and efficiencies. Through analysis, we could see that 0.3 m is an optimal value for the selection of the height bin. Note that the aim of RFC is not to give an exact refractivity profile, but to propose a 'generic' model able to render an accurate approximation of the real atmospheric conditions. From this point of view, RTC is a feasible method of estimating SBD parameters.

5. Conclusion

A novel approach to estimating SBD parameters from surface clutter is presented. Although further studies are necessary to refine this method, the groundwork presented here shows the feasibility of this technique. Though the ray tracing/rank correlation scheme is not accurate enough to perfectly retrieve the refractivity profile, the advantage of this method is the real time working, which makes RTC more attractive for operational use. In this paper, only smooth terrain cases and horizontally homogeneous atmospheric refractivity are discussed; more complex environments will be further considered in future work.

Appendix: Manipulation of the ray tracing equation

On the assumption that the refractive index structure is horizontally homogeneous, the path of a radiowave ray will obey Snell's law in polar coordinates, which is expressed as[17]

$$nr\cos\theta = \text{const.}, \tag{A1}$$

where n is the refractive index of the atmosphere, r is the radial distance from the centre of the Earth to the point under consideration, and θ is the elevation angle made by the ray at the point under consideration. It is clear that

$$r = a_{\mathrm{e}} + z,$$

where a_{e} is the radius of the Earth and z is the vertical distance from the surface of the Earth to the point under consideration. Inserting r into Eq. (A1) leads to

$$n(1 + z/a_{\mathrm{e}})\cos\theta = \text{const.} \tag{A2}$$

Noting that

$$m' = n(1 + z/a_{\mathrm{e}}),$$

then,

$$m'\cos\theta = \text{const.} \tag{A3}$$

For the purposes of numerical calculation, the modified index of refractivity

$$m = n + z/a_{\mathrm{e}}$$

is introduced. In the troposphere, n is approximate to 1 and $z \ll a$,

$$m = n + z/a \approx n + nz/a = n(1 + z/a) = m'. \tag{A4}$$

So Snell's law in the m space could be obtained to be

$$m\cos\theta = \text{const.} \tag{A5}$$

Acknowledgment

The authors would like to thank Professor Peter Gerstoft at Marine Physical Laboratory, University of California, San Diego, La Jolla, California, USA, for providing the Wallops'98 radar clutter data and corresponding helicopter refractivity measurements. The authors would also thank Professor Yan H J for his insight into different layers in discussion.

References

[1] Yan H J, Fu Y and Hong Z J 2006 *Introduction to Modern Atmospheric Refraction* (Shanghai: Science and Educational Press) (in Chinese)

[2] Rowland J R and Babin S M 1987 *Johns Hopkins APL Tech. Dig.* **8** 413

[3] Gersoft P, Rogers L T, Krolik J K and Hodgkiss W S 2003 *Radio Sci.* **38** 8053

[4] Vasudevan S, Anderson R H, Kraut S, Gerstoft P, Rogers L T and Krolik J L 2007 *Radio Sci.* **42** 3423

[5] Yardim C, Gerstoft P and Hodgkiss W S 2008 *IEEE Antennas Propag.* **56** 1058

[6] Douvenot R, Fabbro V, Gerstoft P, Bourlier C and Saillard J 2008 *Radio Sci.* **43** 3842
[7] Sheng Z, Huang S X and Zheng G D 2009 *Acta Phys. Sin.* **58** 4335 (in Chinese)
[8] Liang G and Bertoni H L 1998 *IEEE Antennas Propag.* **46** 853
[9] Erricolo D, Crovella U G and Uslenghi P 2002 *IEEE Antennas Propag.* **50** 736
[10] Sevgi L 2004 *IEEE Antennas and Propaga. Mag.* **46** 140
[11] Rogers L T 1996 *IEEE Antennas Propag.* **44** 460
[12] Barrios A E 2004 *Radio Sci.* **39** 6013
[13] Barrios A E 2003 *Considerations in the Development of the Advanced Propagation Model (APM) For U.S. Navy Applications* AD-A 445 237
[14] Kuttler J R and Dockery G D 1991 *Radio Sci.* **26** 381
[15] Xu W C, Chang C Q, Hung Y S and Fung C W 2008 *IEEE Transactions on Signal Processing* **56** 2239
[16] Huang S X, Zhao X F and Sheng Z 2009 *Chin. Phys.* B **18** 5084
[17] Choi J 1996 *Parametric Error Analysis of Tropospheric Propagation Effects* AD-A 310 468